AIAA Guidance, Navigation, and Control Conference
08 - 11 August 2011, Portland, Oregon

AIAA 2011-6477

Network Topology Design for UAV Swarming with Wind Gusts

Airlie Chapman*, Ran Dai† and Mehran Mesbahi‡
University of Washington, Seattle, WA, 98105, USA

The cornerstone of effective topology design for networked systems is the appreciation of the interplay between system performance and network structure. In this paper, we examine the problem of Unmanned Aerial Vehicle (UAV) swarming in the presence of wind gusts. Firstly, we model an altitude consensus-based leader-follower model exposed to gust disturbances. We then proceed to examine system-theoretic and topological features that promote network disturbance rejection. Specifically the open loop $\mathcal{H}_2$ norm of the system is selected as a performance metric. Its topological features are highlighted via a realization of the open loop $\mathcal{H}_2$ norm in terms the effective resistance of the corresponding electrical network. We subsequently utilize Mixed-Integer Semidefinite Programming (MISDP) to generate the optimal unweighted network to minimize this metric. This is then followed by exploiting the open loop $\mathcal{H}_2$ norm related topological features to design a network rewiring protocol to maximize this metric. Finally, these topology design tools are applied to wind gust rejection in disturbed swarming scenarios, demonstrating the viability of topology-assisted design for improved performance.

I. Introduction

Unmanned Aerial Vehicle (UAV) swarming, the case study of this paper, is an example of a leader-follower model and involves distributing tasks over many small vehicles which can be coordinated by leader UAVs. One of the costs of the decentralized architecture is increased susceptibility of the small vehicles to external disturbances, such as wind gusts. As the swarm is cooperative, disturbances can be inadvertently amplified via coordination between UAVs. Similarly, favorable disturbance correction can be inadvertently dampened. This paper manipulates the UAV coordination network topology to improve the swarm's resilience to wind gusts.

We model the UAV swarming with leader-follower dynamics running a consensus-based protocol with the objective of reaching agreement on altitude. Consensus provides a framework for simple, but effective, distributed information-sharing and control for networked, multi-agent systems in settings such as multi-vehicle control, formation control, swarming, and distributed estimation. See for example, Olfati-Saber et al.[1] and Mesbahi and Egerstedt.[2] One of the popular adaptions of traditional consensus is leader-follower dynamics[3,4] in which leader agents, that do not conform to traditional consensus, can impact the network by exploiting the other agents' consensus dynamics. This can be done intentionally by knowledgeable controllers, for example leader UAVs correcting for wind disturbances, or unintentionally by powerless agents, for example a UAV affected by a wind gust skews the consensus results. In the former case this impact is favorable and in the latter case is detrimental. We investigate the relationship between the network topology and the impact of the leaders' input in a leader-follower system. Topological features are investigated which vary the leaders' impact, measured in terms of the open loop $\mathcal{H}_2$ norm of the system. Favorable network topologies are then designed optimally using a Mixed-Integer Semidefinite Programming (MISDP) framework and suboptimally via a decentralized rewiring protocol, exploiting the aforementioned topological features.

*Graduate Student, Department of Aeronautics and Astronautics, University of Washington, Box 352400, Seattle, WA 98195-2400. Email: airliec@u.washington.edu

†Research Associate, Department of Aeronautics and Astronautics, University of Washington, Box 352400, Seattle, WA 98195-2400. Email: dairan@u.washington.edu

‡Professor, Department of Aeronautics and Astronautics, University of Washington, Box 352400, Seattle, WA 98195-2400. Email: mesbahi@aa.washington.edu

Two specialized cases of wind-gust swarming are considered. The first case is when the UAVs are spread over a large area, for example for *sparse* surveillance of a region, and as such localized wind gusts act on a subset of the UAVs in the swarm. The UAVs are assumed to be equipped with sensors and controllers to perform simple dampening of their measured wind gusts. In the second case, we consider a *dense* swarm formation, for example high-precision ground sensing. A consequence of the UAV's proximity within a dense swarm is that single wind gusts affect all agents in the swarm. For this second case, full state monitoring of all UAVs can be performed by a subset of agents due to the graph's compactness. An $\mathcal{H}_2$ controller (Linear Quadratic Gaussian (LQG) controller) is implemented on leader agents to reject the wind gust disturbance. These motivating examples are dubbed *sparse* and *dense swarming*, respectively.

Aircraft being exposed to wind gusts is a well-researched area.[5,6] Gust-exposed Micro Aerial Vehicles (MAV)[7] on the other hand is an emerging research field and is highly relevant to this paper since the agents used in large-scale swarming are often MAVs. Shyy et al.[8] has investigated biology-inspired MAV design to combat environmental disturbances. A myriad of controllers have been proposed for such a task including $\mathcal{H}_\infty$ controllers[9] and $\mathcal{H}_2$ controllers.[10] One of the few papers that has studied a network-based gust-exposed UAV swarm is Meskin et al.[11] who proposed a hybrid fault-detection and isolation approach involving thresholding between tolerable and large disturbances in the system, ignoring the coordination topology of the UAV swarm. Our approach aims to instead maintain the underlying consensus dynamics and favorably alter the coordination topology.

One of the attractions of networked systems is that system performance is strongly coupled to the underlying network structure. For traditional consensus, system performance and its ties to network structure is a well researched problem where the second smallest eigenvalue of the graph Laplacian is a favored metric to quantify the convergence rate.[4,12] Interest has also been shown with other network measures, for example the largest eigenvalue of the graph Laplacian.[13] However, these metrics prove less attractive in leader-follower consensus where convergence rates can vary dramatically depending on where the leaders are located within the network. For the leader-follower consensus, our selected performance metric is the open loop $\mathcal{H}_2$ norm. The system-theoretic interpretation of this metric provides a more tangible link to system performance in the presence of disturbances and leaders. Further, the equivalent circuit representation of the network provides the presentation of the open loop $\mathcal{H}_2$ norm as the total *effective resistance* of the graph agents.

The open loop $\mathcal{H}_2$ norm is studied when the network system is subjected to disturbances or unknown noise, or when the controllability of the system is a concern. Under such circumstances, reducing the open loop $\mathcal{H}_2$ norm, where the input is from the gust-affected UAVs, will decrease the susceptibility of the system to the gust, and increasing the open loop $\mathcal{H}_2$ norm, where the input is from the leaders, tends to increase the receptiveness of the system to control. Work in this area focuses on allocating the weights on the coordination links between UAVs (the edges of the coordination topology).[14] We examine the topology of the optimal coordination graph that will achieve the minimum and maximum open loop $\mathcal{H}_2$ norm with of nominated leader UAVs, respectively. If the existence or absence of a coordination link between two random UAVs is represented by a Boolean value, the off-diagonal entries of the adjacency matrix can all be expressed by the binary variables one or zero. Our objective is to determine these binary values in order to optimize the performance index.

We address the optimization of the open loop $\mathcal{H}_2$ norm on two fronts. The first uses Mixed-Integer Semidefinite Programming[15] to minimize the metric under network connectivity constraints to produce the optimal graph. Unfortunately, maximizing the metric in an optimization setting is NP-hard (a provably intractable problem) and we propose a suboptimal decentralized protocol to improve this metric. Our approach is to perform edge trades among neighboring agents within the network that tend to increase the total effective resistance of the graph and consequently the open loop $\mathcal{H}_2$ norm.

The general area of designing topologies to optimize for certain metrics has been addressed by many authors: Ghosh and Boyd[16] maximized the second smallest eigenvalue of the graph Laplacian, Zelazo and Mesbahi[17] optimized the network $\mathcal{H}_2$ performance where the graph is not in the closed loop of the dynamics, Wan et al.[18] maximized the largest eigenvalue of the graph Laplacian. All aforementioned authors used optimization techniques over *weighted* graphs. Kim and Mesbahi[19] used power functions to approximately represent the on/off linkage relationship when searching for the maximum second-smallest eigenvalue of the Laplacian to increase convergence speeds of the network dynamics. Wu and Wang[20] has approach the same problem using genetic-algorithms. Intuitive based methods of network reconfiguration have been designed to improve network resilience, for example using thresholding methods to decide when to alter the topology.[21]

The paper is organized as follows. §II contains the problem formulation and relevant background. Two

models for a UAV swarm exposed to wind gusts are also introduced in §II. An analysis of the open loop $\mathcal{H}_2$ norm is presented in §IV and its relationship to system performance and the effective resistance of the network is established. In §IV, two methods are proposed to design network topologies optimized for the open loop $\mathcal{H}_2$ norm and conducive to wind-gust disturbance rejection. We conclude the paper with a few remarks in §V.

II. Background and Model

We provide a brief background on the models that will be used in this paper, including abbreviated descriptions on graphs and the consensus protocol in both its traditional and leader-follower versions. First we introduce the notation: $\|\cdot\|_2$ and $\|\cdot\|_\infty$ denote the Euclidean and infinity norms, respectively; $\mathbf{tr}(\cdot)$ denotes the trace of a matrix; $|\cdot|$ denotes the cardinality of a set; $\mathbf{1}$ denotes the column vector of ones; $\otimes$ denotes the Kronecker product. The spectrum of matrix $M \in \mathbb{R}^{n\times n}$ is denoted and ordered as $\lambda_1(M) \leq \lambda_2(M) \leq \cdots \leq \lambda_n(M)$. For matrices $M, N \in \mathbb{R}^{n\times n}$, we write $N \preceq M$ if $M - N$ is positive semidefinite.

An undirected graph $\mathcal{G} = (V, E)$ is defined by a node set V with cardinality n, the number of nodes in the graph, and an edge set E comprised of pairs of nodes, where nodes v_i and v_j are adjacent if $\{v_i, v_j\} \in E \subseteq [V]^2$.[a] A special family of graphs is tree graphs $\mathcal{T}$ where all two node pairs are connected by exactly one simple path, i.e., a connected graph without cycles.

We denote the set of nodes adjacent to v_i as $\mathcal{N}(v_i)$ and the minimum path length, induced by the graph $\mathcal{G}$, between nodes v_i and v_j as $d(v_i, v_j)$. The degree δ_i of node v_i is the number of its adjacent nodes. The degree matrix $\Delta(\mathcal{G}) \in \mathbb{R}^{n\times n}$ is a diagonal matrix with δ_i at position (i, i). The adjacency matrix is a $n \times n$ symmetric matrix with $[\mathcal{A}(\mathcal{G})]_{ij} = 1$ when $\{v_i, v_j\} \in E$ and $[\mathcal{A}(\mathcal{G})]_{ij} = 0$ otherwise. The combinatorial Laplacian is defined as $L(\mathcal{G}) = \Delta(\mathcal{G}) - \mathcal{A}(\mathcal{G}) \in \mathbb{R}^{n\times n}$ which is a (symmetric) positive semi-definite matrix.

Now consider $x_i(t) \in \mathbb{R}$ to be the i-th node's (or for our case agent's) state at time t. The continuous-time consensus protocol is defined as

$$\dot{x}_i(t) = \sum_{\{v_i, v_j\} \in E} (x_j(t) - x_i(t)) . \tag{1}$$

In a compact form with $x(t) \in \mathbb{R}^n$, the collective dynamics is represented as $\dot{x}(t) = -L(\mathcal{G})x(t)$ with $L(\mathcal{G})$ being the Laplacian of the underlying interaction topology.[1]

We next introduce a model for leader-follower consensus over a graph $\breve{\mathcal{G}} = (\breve{V}, \breve{E})$ associated with a pair $\mathcal{R} = (R, \mathcal{E}_R)$, where $R \in \breve{V}$ is the cardinality r leader agents set and $\mathcal{E}_R \subseteq \breve{E}$ is the set of edges used by the leader agents to inject signals into the network. It is assumed that for a leader agent $r_j \in R$ the same signal $u_j(t) \in \mathbb{R}$ is delivered along every edge adjacent to it. The remaining edges and agents of $\breve{\mathcal{G}}$ form the subgraph $\mathcal{G}$, with the exception of those edges between leaders which are removed. This assumption is justified as we assume leaders are working cooperatively and do not required coupled dynamics of the other leaders' states. Figure 1 provides a graphical representation of this notation and setup.

The resulting leader-follower system now assumes the form,

$$\dot{x}_i(t) = \sum_{\{v_i, v_j\} \in E} (x_j(t) - x_i(t)) + \sum_{\{v_i, r_j\} \in \mathcal{E}_R} (u_j(t) - x_i(t)) : \tag{2}$$

with full dynamics

$$\dot{x}(t) = A(\mathcal{G}, \mathcal{R})x(t) + B(\mathcal{R})u(t), \tag{3}$$

where $B(\mathcal{R}) \in \mathbb{R}^{n\times r}$ with $[B(\mathcal{R})]_{ij} = 1$ when $\{r_j, v_i\} \in \mathcal{E}_R$ and $[B(\mathcal{R})]_{ij} = 0$ otherwise, and

$$A(\mathcal{G}, \mathcal{R}) = -\left(L(\mathcal{G}) + D(\mathcal{R})\right) \in \mathbb{R}^{n\times n}, \tag{4}$$

where $D(\mathcal{R}) \in \mathbb{R}^{n\times n}$ with $[D(\mathcal{R})]_{ii} = \delta_i^r$ where δ_i^r is the number of leaders adjacent to v_i and $[D(\mathcal{R})]_{ij} = 0$ otherwise. We define δ_j^v as the number of follower agents adjacent to r_j. We distinguish two special cases of this setup: one in which there is exactly one leader for each edge $\mathcal{E}_R$ and so a *distinct* control signal is delivered through each edge, denoted with the leader pair $\mathcal{R}_d$, and one where there exists only one leader node so a *common* signal is delivered through each edge of $\mathcal{E}_R$, denoted with pair $\mathcal{R}_c$. A sample model and

[a] The notation $[V]^2$ refers to the set of two-element subsets of V.

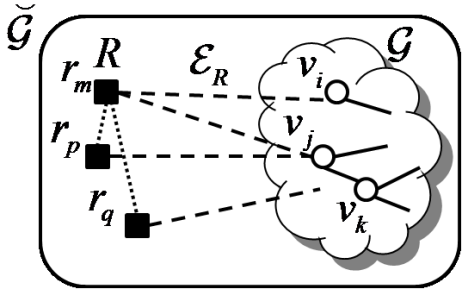

Figure 1. Example of leader-follower notation. The leaders in set R are connected to the followers in V via the edges $\mathcal{E}_R$. The followers V with coordination edges E form a graph $\mathcal{G}$ (some of which is depicted in the image with agents v_i, v_j, v_k and solid edges). Edges between leaders (dotted) can be ignored and followers. The complete leader and follower graph containing all agents $\breve{V}$ and edges $\breve{E}$ is denoted as $\breve{\mathcal{G}}$.

its system matrices as well as the special cases of $\mathcal{R}_d$ and $\mathcal{R}_c$ are depicted in Figure 2. We also denote the set of agents v_i such that $\{r_j, v_i\} \in \mathcal{E}_R$ by $\pi(\mathcal{E}_R)$. In other words, $\pi(\mathcal{E}_R)$ is simply the set of agents that directly connect to leader agents.

We recognize $A(\mathcal{G}, \mathcal{R})$ in Equation (4) as the Dirichlet matrix, or grounded Laplacian.[22,23] The spectrum of $A(\mathcal{G}, \mathcal{R})$ relates closely to the spectrum of $L(\mathcal{G})$. In this way, the structure of the underlying graph is related to the dynamics of model (3). In the next section we proceed to disturb the leader-follower system with a wind gust. Before this an auxiliary observation about the Dirichlet matrix, to be used subsequently, is the following.

Proposition 1. [24] *The matrix $A(\mathcal{G}, \mathcal{R})$ of model (3) is negative definite (and so invertible) if the original graph is connected.*

The following is the characterization of the wind gust in state space form which will be subsequently used in the swarming models.

A. Wind Model

A vertical wind gust w_g is not white, but has a power spectral density given in Dryden form[5] as

$$\Phi_w(\omega) = 2L\sigma^2 \frac{1 + 3L^2\omega^2}{(1 + L^2\omega^2)^2}, \tag{5}$$

with w the frequency in rad/s, σ the turbulence intensity, and L the turbulence scale length divided by true airspeed.

The power spectral density (5) can be factored[5] as,

$$\Phi_w(s) = H_w(s)H_w(-s),$$

where

$$H_w(s) = \sigma\sqrt{\frac{6}{L}} \frac{s + 1/L\sqrt{3}}{s^2 + 2s/L + 1/L^2}.$$

Now a realization of $H_w(s)$ corresponding to w, a white noise input with zero mean and unit variance W, is given by

$$\begin{aligned} \dot{z}(t) &= \begin{bmatrix} 0 & 1 \\ -\frac{1}{L^2} & -\frac{2}{L} \end{bmatrix} z(t) + \begin{bmatrix} 0 \\ 1 \end{bmatrix} w(t), \\ &= A_w z(t) + B_w w(t) \end{aligned} \tag{6}$$

where $z(t) \in \mathbb{R}^2$ are the internal states of the wind gust and

$$\begin{aligned} w_g(t) &= \gamma \begin{bmatrix} \frac{1}{L\sqrt{3}} & 1 \end{bmatrix} z(t) \\ &= C_w z(t) \end{aligned} \tag{7}$$

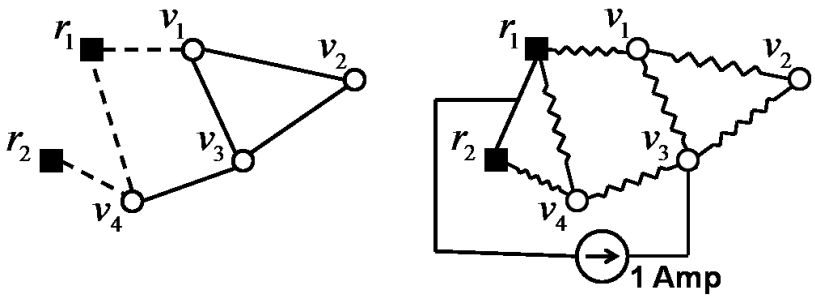

(a) (b)

$$A(\mathcal{G},\mathcal{R}) = \begin{bmatrix} -3 & 1 & 1 & 0 \\ 1 & -2 & 1 & 0 \\ 1 & 1 & -3 & 1 \\ 0 & 0 & 1 & -3 \end{bmatrix}, \; B(\mathcal{R}) = \begin{bmatrix} 1 & 0 \\ 0 & 0 \\ 0 & 0 \\ 1 & 1 \end{bmatrix}$$

$$\text{(c) } B(\mathcal{R}_d) = \begin{bmatrix} 1 & 0 & 0 \\ 0 & 0 & 0 \\ 0 & 0 & 0 \\ 0 & 1 & 1 \end{bmatrix}, \; B(\mathcal{R}_c) = \begin{bmatrix} 1 \\ 0 \\ 0 \\ 2 \end{bmatrix}$$

Figure 2. (a) Network graph with leader (control) agents r_1 and r_2 attached to agents v_1 and v_4, leading to an altered Laplacian $A(\mathcal{G},\mathcal{R})$ and input matrix $B(\mathcal{R})$ of model (3). (b) Equivalent electrical network. The potential difference $V_{v_3} - V_{\mathcal{R}}$ is the effective resistance between v_3 and common resistor node $\{r_1, r_2\}$. (c) The control matrices relating to the special cases of distinct and common control.

where $\gamma = \sigma\sqrt{6/L}$.

We can now proceed to formulate the full UAV swarming scenarios and incorporate the wind model dynamics.

B. Swarming Models

We present two swarming models with the objective of reaching and maintaining a common altitude among a network (swarm) of UAVs by using the consensus protocol (1). In the first model we consider the swarm being spread over a large area. Due to the large separation of vehicles, different wind gusts affect agents in isolation. Basic gust correction is present on each UAV which has the effect of dampening their wind gust. This model is dubbed *sparse swarming*. The second model examines a swarm grouped together over a small area. Wind gusts no longer act on agents in isolation but affect all agents in the swarm simultaneously. A set of control UAVs (leaders) that can monitor all follower UAVs are introduced and integrated into the consensus dynamics. These control UAVs have onboard altitude maintenance and vary their altitudes so as to correct for such disturbances in the swarm through the consensus dynamics. This model is dubbed *dense swarming*.

For both models, the swarm of UAVs contains a subset of follower UAVs. Each follower examines the relative altitude of vehicles in their neighborhood, via onboard relative altitude sensors, and applies the consensus protocol. The remaining UAVs are considered leader agents which do not obey the consensus protocol, the reason for which distinguishes our two models. For sparse swarming, the gust-affected agents, which are the leaders in this case, *inadvertently* disobey the consensus protocol as each are instead dampening their individual wind gusts. In dense swarming, the leaders are special controller UAVs that are *actively* ignoring the protocol with the objective to correct for wind gusts that are perturbing the velocities of the followers in the network. We subsequently model, for both swarming scenarios, each follower agent as a single integrator with dynamics dictated by the consensus algorithm for altitude alignment. The follower altitude states are $x(t)$ and the leader states are $q(t)$ and $u(t)$ for the sparse and dense swarming models, respectively. The zero altitude ($x(t) = 0$, $q(t) = 0$ and $u(t) = 0$) can be selected arbitrarily, which for simplicity can be set such that $x(0) = 0$, $q(t) = 0$ and $u(0) = 0$. We now proceed to present our two swarming models for

sparse and dense swarming.

1. *Sparse Swarming*

In sparse swarming, we assume distinct gusts act upon r UAVs of the network. Each UAV has the same capability to perform basic gust correction. They are each equipped with sensors and actuators that can measure and dampen the local wind gust. The subsequent altitude dynamics $q(t) \in \mathbb{R}^r$ of the gust are modeled by

$$q(t) = \bar{h}\omega_g(t) + \bar{x}(0)$$

where $\bar{h} \in \mathbb{R}$ is the dampening effect (common to all UAVs) of the wind gusts $\omega_g(t) \in \mathbb{R}^r$ and $\bar{x}(0) \in \mathbb{R}^r$ is the altitudes of the affected UAVs before the gusts hit.

Incorporating the filter dynamics of Equation (6) with filter state $z_i(t) \in \mathbb{R}^2$ and white noise $w_i(t) \in \mathbb{R}$ corresponding to gust $[\omega_g(t)]_i$, $\zeta(t) = \left[z_1(t)^T, \ldots, z_r(t)^T\right]^T \in \mathbb{R}^{2r}$ and $\xi(t) = [w_1(t), \ldots, w_r(t)]^T \in \mathbb{R}^r$ then

$$\begin{aligned}
\begin{bmatrix} \dot{x}(t) \\ \dot{\zeta}(t) \end{bmatrix} &= \begin{bmatrix} A(\mathcal{G},\mathcal{R})x(t) + B(\mathcal{R})q(t) \\ \dot{\zeta}(t) \end{bmatrix} \\
&= \begin{bmatrix} A(\mathcal{G},\mathcal{R})x(t) + B(\mathcal{R})\left(\bar{h}\omega_g(t) + \bar{x}(0)\right) \\ \dot{\zeta}(t) \end{bmatrix} \\
&= \begin{bmatrix} A(\mathcal{G},\mathcal{R})x(t) \\ \dot{\zeta}(t) \end{bmatrix} + \begin{bmatrix} \bar{h}B(\mathcal{R}) \\ 0 \end{bmatrix} (I_{r\times r} \otimes C_w)\,\zeta(t) + \begin{bmatrix} B(\mathcal{R})\bar{x}(0) \\ 0 \end{bmatrix} \\
&= \begin{bmatrix} A(\mathcal{G},\mathcal{R})x(t) \\ (I_{r\times r} \otimes A_w)\,\zeta(t) + (I_{r\times r} \otimes B_w)\,\xi(t) \end{bmatrix} + \begin{bmatrix} \bar{h}B(\mathcal{R})\,(I_{r\times r} \otimes C_w) \\ 0 \end{bmatrix} \zeta(t) + \begin{bmatrix} B(\mathcal{R})\bar{x}(0) \\ 0 \end{bmatrix} \\
&= \begin{bmatrix} A(\mathcal{G},\mathcal{R}) & \bar{h}B(\mathcal{R})\,(I_{r\times r} \otimes C_w) \\ 0 & (I_{r\times r} \otimes A_w) \end{bmatrix} \begin{bmatrix} x(t) \\ \zeta(t) \end{bmatrix} + \begin{bmatrix} 0 \\ (I_{r\times r} \otimes B_w) \end{bmatrix} \xi(t) + \begin{bmatrix} B(\mathcal{R})\bar{x}(0) \\ 0 \end{bmatrix}. \qquad (8)
\end{aligned}$$

We now make the simplifying assumption for modeling that $q(t)$ are arbitrary. For simulation results, we will use the full dynamics in Equation 8.

Noting that all the non-gust-affected UAVs (followers) states $x(t)$ are of interest, the dynamics can be represented as

$$\begin{aligned}
\dot{x}(t) &= A(\mathcal{G},\mathcal{R})x(t) + B(\mathcal{R})q(t) := \mathcal{A}_S x(t) + \mathcal{B}_S q(t) \qquad (9) \\
y(t) &= \mathcal{C}_S x(t),
\end{aligned}$$

where $y(t) \in \mathbb{R}^n$ is the controller observations, $\mathcal{C}_S = I_{n\times n}$, and $\mathcal{A}_S$ and $\mathcal{B}_S$ are apparent from Equation 9

The objective of the paper is to adapt the coordination topology $\mathcal{G}$ and $\mathcal{R}$ to reduce the network amplification of the locally-dampened wind gust $q(t)$ on the altitude of the non-gust affected vehicles $y(t)$. In other words, for a fixed $\bar{x}(0)$, to dampen the input to output mapping of $q(t)$ to $y(t)$.

2. *Dense Swarming*

The assumptions for the dense swarming model are that a controller corresponding to the leader's states $u(t) \in \mathbb{R}^r$ is present and that the same gust $w_g(t) \in \mathbb{R}$ acts upon all agents in the network. Then the full dynamics are

$$\begin{aligned}
\begin{bmatrix} \dot{x}(t) \\ \dot{z}(t) \end{bmatrix} &= \begin{bmatrix} A(\mathcal{G},\mathcal{R})x(t) + B(\mathcal{R})u(t) \\ \dot{z}(t) \end{bmatrix} + \begin{bmatrix} H \\ 0 \end{bmatrix} w_g(t) \\
&= \begin{bmatrix} A(\mathcal{G},\mathcal{R})x(t) \\ A_w z(t) + B_w w(t) \end{bmatrix} + \begin{bmatrix} B(\mathcal{R}) \\ 0 \end{bmatrix} u(t) + \begin{bmatrix} H \\ 0 \end{bmatrix} C_w z(t) \\
&= \begin{bmatrix} A(\mathcal{G},\mathcal{R})x(t) \\ A_w z(t) + B_w w(t) \end{bmatrix} + \begin{bmatrix} B(\mathcal{R}) \\ 0 \end{bmatrix} u(t) + \begin{bmatrix} A_z \\ 0 \end{bmatrix} z(t) \\
&= \begin{bmatrix} A(\mathcal{G},\mathcal{R}) & HC_w \\ 0 & A_w \end{bmatrix} \begin{bmatrix} x(t) \\ z(t) \end{bmatrix} + \begin{bmatrix} B(\mathcal{R}) \\ 0 \end{bmatrix} u(t) + \begin{bmatrix} 0 \\ B_w \end{bmatrix} w(t) \qquad (10)
\end{aligned}$$

where $H = [h_1, \ldots, h_n]^T$ and $h_i \in \mathbb{R}$ is a scaling factor specific to UAV i's gust-vehicle interaction.

We assume that the agent states of the system can all be sensed with some measurement noise $v(t) \in \mathbb{R}^n$ which is a white noise vector with correlation matrix $V \in \mathbb{R}^{n \times n}$. Restating Equation (10) in compact form, we have

$$\begin{aligned} \begin{bmatrix} \dot{x}(t) \\ \dot{z}(t) \end{bmatrix} &= \mathcal{A}_D \begin{bmatrix} x(t) \\ z(t) \end{bmatrix} + \mathcal{B}_D u(t) + G_D w(t) \\ y(t) &= \mathcal{C}_D \begin{bmatrix} x(t) \\ z(t) \end{bmatrix} + v(t), \end{aligned} \tag{11}$$

where $\mathcal{A}_D$, $\mathcal{B}_D$ and G_D are apparent from Equation (10), $y(t) \in \mathbb{R}^n$ is the controller observations of which we assume the leaders can observe all the followers' velocities and so $\mathcal{C}_D = \begin{bmatrix} I_{n\times n} & 0_{n\times 2} \end{bmatrix}$.

The objective of the paper, explored further in the next section, is to adapt the coordination topology $\mathcal{G}$ and $\mathcal{R}$ to increase the amplification of the control input $u(t)$ on the altitude of all UAVs $y(t)$. In other words, to amplify the input to output mapping of $u(t)$ to $y(t)$. To quantify the amplification of $u(t)$ to $y(t)$ as well as the dampening of $q(t)$ to $y(t)$ we use the open loop $\mathcal{H}_2$ norm of the system, which will be discussed in the following section.

III. Open Loop $\mathcal{H}_2$ Norm

As a group of networked UAVs do not require physical interconnections for their coordinated behavior, they have the advantage that their inter-vehicle coordination graph can be *rewired*. This observation leads us into our next form of gust correction, namely via topology design. We present a system-theoretic metric that can be exploited to adapt the network topology with the objective of improving the nominal $\mathcal{H}_2$ performance. The open loop $\mathcal{H}_2$ norm of the system proves to be particularly suitable for such an analysis. For a system of the form

$$\begin{aligned} \dot{x}(t) &= Ax(t) + Bu(t) \\ y(t) &= Cx(t) + Du(t), \end{aligned}$$

the open loop $\mathcal{H}_2$ norm can be defined in term of the controllability gramian, $P_T(A,B) := \int_0^T e^{A\tau} B B^T e^{A^T \tau} d\tau$ for the system. The square of open loop $\mathcal{H}_2$ norm is

$$\|G(s)\|_2^2 = \mathbf{tr}\left(C P_\infty(A,B) C^T\right), \tag{12}$$

where the state-space realization is $G(s) = C(sI - A)^{-1} B$.

b) The energy of the states at the output from a unit impulse input u when $x(0) = 0$ is

$$\int_0^\infty x(t)^T x(t) dt = \|G(s)\|_2^2.$$

From these observations we can state that inputs perturb the outputs more as $\|G(s)\|_2$ increases. With this in mind we are motivated to generate network topologies that increase this scalar metric when the leader inputs $u(t)$ are favorable as in model (11) where the leaders correcting for wind disturbances in the network and decrease this metric for unfavorable gust related inputs $q(t)$ as in model (9) where the leaders are delivering adverse wind gusts into the network. Before proceeding with the network generation we examine some properties of $\|G(s)\|_2$ with respect to our specific models (9) and (11). For esthetics, we will present results and optimize for the square of the open loop $\mathcal{H}_2$ norm $\|G(s)\|_2^2$ but make the observation that maximizing or minimizing $\|G(s)\|_2^2$ inadvertently maximizes and minimizes $\|G(s)\|_2$.

In our sparse swarming model (9), if we consider the wind gust effect is analogous to a control input we can formulate the system's controllability gramian and corresponding $\|G(s)\|_2$. The related gramian and $\|G(s)\|_2$ for the sparse and dense swarming models are presented in the following proposition.

Proposition 2. *The controllability gramian as $t \to \infty$ corresponding to model (9) from input $q(t)$ to output $y(t)$ is*

$$P_\infty\left(\mathcal{A}_S, \mathcal{B}_S\right) = P_\infty(A(\mathcal{G},\mathcal{R}), B(\mathcal{R})),$$

and corresponding to model (11) *from input* $u(t)$ *to output* $y(t)$ *is*

$$P_\infty\left(\mathcal{A}_D, \mathcal{B}_D\right) = \begin{bmatrix} P_\infty(A(\mathcal{G},\mathcal{R}), B(\mathcal{R})) & 0 \\ 0 & 0 \end{bmatrix},$$

consequently the wind gust related states are uncontrollable. Thus for, $G_S(s) = \mathcal{C}_S\left(sI - \mathcal{A}_S\right)^{-1}\mathcal{B}_S$ *and* $G_D(s) = \mathcal{C}_D\left(sI - \mathcal{A}_D\right)^{-1}\mathcal{B}_D$ *then* $\|G_S(s)\|_2^2 = \|G_D(s)\|_2^2 = \mathbf{tr}(P_\infty(A(\mathcal{G},\mathcal{R}), B(\mathcal{R})))$.

Proof. The sparse models results follows directly from the definition of the controllability gramian and Equation (12). The matrix $P_\infty\left(\mathcal{A}_D, \mathcal{B}_D\right)$ is the controllability gramian and therefore $\mathcal{A}_D P_\infty\left(\mathcal{A}_D, \mathcal{B}_D\right) + P_\infty\left(\mathcal{A}_D, \mathcal{B}_D\right)\mathcal{A}_D^T = -\mathcal{B}_D\mathcal{B}_D^T$, and so

$$\begin{aligned}
&\mathcal{A}_D \begin{bmatrix} P_\infty(A(\mathcal{G},\mathcal{R}), B(\mathcal{R})) & 0 \\ 0 & 0 \end{bmatrix} + \begin{bmatrix} P_\infty(A(\mathcal{G},\mathcal{R}), B(\mathcal{R})) & 0 \\ 0 & 0 \end{bmatrix}\mathcal{A}_D^T \\
&= \begin{bmatrix} A(\mathcal{G},\mathcal{R}) & A_z \\ 0 & A_w \end{bmatrix}\begin{bmatrix} P_\infty(A(\mathcal{G},\mathcal{R}), B(\mathcal{R})) & 0 \\ 0 & 0 \end{bmatrix} + \begin{bmatrix} P_\infty(A(\mathcal{G},\mathcal{R}), B(\mathcal{R})) & 0 \\ 0 & 0 \end{bmatrix}\begin{bmatrix} A(\mathcal{G},\mathcal{R})^T & 0 \\ A_z^T & A_w^T \end{bmatrix} \\
&= \begin{bmatrix} A(\mathcal{G},\mathcal{R})P_\infty(A(\mathcal{G},\mathcal{R}), B(\mathcal{R})) + P_\infty(A(\mathcal{G},\mathcal{R}), B(\mathcal{R}))A(\mathcal{G},\mathcal{R})^T & 0 \\ 0 & 0 \end{bmatrix} \\
&= \begin{bmatrix} -B(\mathcal{R})B(\mathcal{R})^T & 0 \\ 0 & 0 \end{bmatrix} \\
&= -\begin{bmatrix} B(\mathcal{R}) \\ 0 \end{bmatrix}\begin{bmatrix} B(\mathcal{R})^T & 0 \end{bmatrix} \\
&= -\mathcal{B}_D\mathcal{B}_D^T.
\end{aligned}$$

Applying Equation 12 the proposition follows. □

From Proposition 2, the open loop $\mathcal{H}_2$ norm is common to both sparse and dense swarming models. The distinct difference is that the $\mathcal{H}_2$ norm of interest for the sparse model is mapping the dampened wind gust $q(t)$ to the output $y(t)$ and for the dense model the leader control $u(t)$ to the output $y(t)$. We will henceforth refer to this metric as $\|G_{\mathcal{G},\mathcal{R}}(s)\|_2$ as it is solely dependent on $\mathcal{G}$ and $\mathcal{R}$. Similarly, we will denote $P_\infty(A(\mathcal{G},\mathcal{R}), B(\mathcal{R}))$ as $P(\mathcal{G},\mathcal{R})$.

Directly from the definition of the controllability gramian, one has

$$\begin{aligned}
\|G_{\mathcal{G},\mathcal{R}}(s)\|_2^2 &= \mathbf{tr}\left(\int_0^\infty e^{A(\mathcal{G},\mathcal{R})\tau} B\left(\mathcal{R}\right) B\left(\mathcal{R}\right)^T e^{A(\mathcal{G},\mathcal{R})^T\tau} d\tau\right) \qquad (13)\\
&= \mathbf{tr}\left(B\left(\mathcal{R}\right) B\left(\mathcal{R}\right)^T \int_0^\infty e^{2A(\mathcal{G},\mathcal{R})\tau} d\tau\right) \\
&= -\frac{1}{2}\mathbf{tr}\left(M\left(\mathcal{R}\right) A(\mathcal{G},\mathcal{R})^{-1}\right), \qquad (14)
\end{aligned}$$

where $M\left(\mathcal{R}\right) = B\left(\mathcal{R}\right) B\left(\mathcal{R}\right)^T$.

We make a preliminary remark before proceeding further. It has previously been established that the diagonal of the matrix $-A(\mathcal{G},\mathcal{R})^{-1}$, where $A(\mathcal{G},\mathcal{R})$ is the Dirichlet matrix in (3), has a resistive electrical network interpretation.[22] In this setup, the agents V and R, defined in §II, represent respectively, connection points between resistors corresponding to the edges E and $\mathcal{E}_R$. In addition, all connection points corresponding to the set R are electrically shorted. The effective resistance between two connection points in an electrical network is defined as the potential drop between the two points, when a 1 Amp current source is connected across the two points. The i-th diagonal element of $-A(\mathcal{G},\mathcal{R})^{-1}$ is the effective resistance $E_{\text{eff}}\left(v_i\right)$

between the common shorted external agents R and v_i. An example of the equivalent electrical network is displayed in Figure 2.

We proceed to analyze this metric for our two special leader-agent cases; with $|R| = |\mathcal{E}_R|$ and $|R| = 1$ corresponding to $\mathcal{R}_d$ and $\mathcal{R}_c$ (defined in §II), respectively.

Proposition 3. *For a connected graph $\mathcal{G}$, if each leader agent has exactly one edge and so each edge in $\mathcal{R}_d$ can have an independent signal then,*

$$\|G_{\mathcal{G},\mathcal{R}_d}(s)\|_2^2 = \frac{1}{2} \sum_{v_i \in \pi(\mathcal{E}_R)} E_{\mathit{eff}}(v_i)\,. \tag{15}$$

Proof. We note that $M(\mathcal{R}_d)$ is a diagonal matrix with $[M(\mathcal{R}_d)]_{ii} = 1$ if $v_i \in \pi(\mathcal{E}_R)$ and $[M(\mathcal{R}_d)]_{ii} = 0$, otherwise. Therefore

$$[M(\mathcal{R}_d)\, A(\mathcal{G},\mathcal{R}_d)^{-1}]_{ii} = \begin{cases} [A(\mathcal{G},\mathcal{R}_f)^{-1}]_{ii} & \text{if } v_i \in \pi(\mathcal{E}_R) \\ 0 & \text{otherwise.} \end{cases}$$

From (14) and the effective resistance interpretation of $\left[A(\mathcal{G},\mathcal{R}_f)^{-1}\right]_{ii}$, the statement of the lemma now follows. □

Proposition 4. *For a connected graph $\mathcal{G}$, and all agents apply the same signal then*

$$\|G_{\mathcal{G},\mathcal{R}_c}(s)\|_2^2 = \frac{1}{2}\,|\mathcal{E}_R|\,.$$

Proof. We have $B(\mathcal{R}_c) = B(\mathcal{R}_d)\mathbf{1}_u$ and $A(\mathcal{G},\mathcal{R})^{-1}B(\mathcal{R}_c) = A(\mathcal{G},\mathcal{R})^{-1}B(\mathcal{R}_d)\mathbf{1}_u = -\mathbf{1}_x$ hence

$$\begin{aligned} \mathbf{tr}\left(M(\mathcal{R})\int_0^\infty e^{2A(\mathcal{G},\mathcal{R})\tau}d\tau\right) &= \mathbf{tr}\left(B(\mathcal{R}_c)^T A(\mathcal{G},\mathcal{R})^{-1}B(\mathcal{R}_c)\right) \\ &= \mathbf{tr}\left(\mathbf{1}_u^T B(\mathcal{R}_d)^T \mathbf{1}_x\right) = |\mathcal{E}_R|\,. \end{aligned}$$

From (14) , the statement of the lemma now follows. □

Corollary 5. *For a graph $\breve{\mathcal{G}}$ and model* (3) *with one leader,*

$$\|G_{\mathcal{G},\mathcal{R}}(s)\|_2^2 = \frac{1}{2}\delta(r_1),$$

where $\delta(r_1)$ is the degree of the leader in the graph $\breve{\mathcal{G}}$.

Proof. The statement of the corollary follows directly from Proposition 4. □

Remark 6. The implication of Corollary 5 is that for the case of a single leader, selecting the agent within the network with the highest degree will maximize the open loop $\mathcal{H}_2$ norm of the system, regardless of the structure of the network.

We now relate the controllability gramian of a generic $\mathcal{R}$ with the controllability gramians of special cases of $\widetilde{\mathcal{R}}_d$ and $\widetilde{\mathcal{R}}_c$. We design these special leader sets cases such that: a control u_c of system $\widetilde{\mathcal{R}}_c$ maps to a control u of system $\mathcal{R}$ so that $B(\widetilde{\mathcal{R}}_c)u_c = B(\mathcal{R})u$ when $H_1 u_c = u$ and so that $\|u_c\|_2 = 1 \implies \|u\|_2 = 1$, for some H_1. Similarly, $B(\mathcal{R})u = B(\widetilde{\mathcal{R}}_d)u_d$ when $H_2 u = u_d$ and so that $\|u\|_2 = 1 \implies \|u_d\|_2 = 1$, for some H_2. This corresponds to $B(\mathcal{R}) = B(\widetilde{\mathcal{R}}_d)H_2$, $B(\widetilde{\mathcal{R}}_c) = B(\mathcal{R})H_1$, where $H_1 = \frac{1}{\sqrt{|R|}}\mathbf{1} \in \mathbb{R}^{|R|\times 1}$, $H_2 \in \mathbb{R}^{|R_d|\times|R|}$ and

$$[H_2]_{ij} = \begin{cases} \frac{1}{\sqrt{\delta_j^v}} & \text{if } (r_j, v_i) \in \mathcal{E}_R \\ 0 & \text{otherwise.} \end{cases}$$

Therefore,

$$\left[B(\widetilde{\mathcal{R}}_c)\right]_i = \begin{cases} \frac{n_i}{\sqrt{|R|}} & \text{if } (r_j, v_i) \in \mathcal{E}_R \\ 0 & \text{otherwise,} \end{cases}$$

and

$$\left[B(\widetilde{\mathcal{R}}_d)\right]_{ij} = \begin{cases} \sqrt{\delta_j^v} & \text{if } (r_j, v_i) \in \mathcal{E}_R \\ 0 & \text{otherwise.} \end{cases}$$

Proposition 7. *For a graph $\mathcal{G}$ and the leader sets defined above for $\widetilde{\mathcal{R}}_c$ and $\widetilde{\mathcal{R}}_d$,*

$$P(\mathcal{G}, \widetilde{\mathcal{R}}_c) \preceq P(\mathcal{G}, \mathcal{R}) \preceq P(\mathcal{G}, \widetilde{\mathcal{R}}_d).$$

Proof. We note that by design for every $\|u_c\|_2 = 1$ there exists a $\|u\|_2 = 1$ such that $\left|B(\widetilde{\mathcal{R}}_c)u_c\right|_2 \leq |B(\mathcal{R})u|_2$ and similarly for every $\|u\|_2 = 1$ there exists a $\|u_d\|_2 = 1$ such that $|B(\mathcal{R})u_c|_2 \leq \left|B(\widetilde{\mathcal{R}}_d)u\right|_2$. The statement of the proposition follows. □

Lemma 8. *For a graph $\mathcal{G}$ and leader set $\mathcal{R}$,*

$$\frac{1}{2\,|R|}\,|\mathcal{E}_R| \leq \|G_{\mathcal{G},\mathcal{R}}(s)\|_2^2 \leq \frac{1}{2} \sum_{v_i \in \pi(\mathcal{E}_R)} \alpha_i E_{\mathit{eff}}(v_i)\,,$$

where

$$\alpha_i = \sum_{(r_j, v_i) \in \mathcal{E}_R} \delta_j^v,$$

i.e., α_i is the sum of the non-leader degrees for each leader attached to v_i.

Proof. From Proposition 7,

$$\left\|G_{\mathcal{G},\tilde{\mathcal{R}}_c}(s)\right\|_2^2 \leq \|G_{\mathcal{G},\mathcal{R}}(s)\|_2^2 \leq \left\|G_{\mathcal{G},\tilde{\mathcal{R}}_d}(s)\right\|_2^2,$$

and

$$\begin{aligned} \mathbf{tr}\left(P(\mathcal{G}, \widetilde{\mathcal{R}}_c)\right) &= \mathbf{tr}\left(B(\widetilde{\mathcal{R}}_c)^T A(\mathcal{G}, \mathcal{R})^{-1} B(\widetilde{\mathcal{R}}_c)\right) \\ &= \frac{1}{|R|}\mathbf{tr}\left(B(\mathcal{R}_c)^T A(\mathcal{G}, \mathcal{R})^{-1} B(\mathcal{R}_c)\right) \\ &= \frac{1}{|R|}\mathbf{tr}\left(P(\mathcal{G}, \mathcal{R}_c)\right). \end{aligned}$$

We note that $M(\mathcal{R}_d)$ is a diagonal matrix with $[M(\mathcal{R}_d)]_{ii} = \delta_j^v$ if $(r_j, v_i) \in \mathcal{E}_R$ and $[M(\mathcal{R}_d)]_{ii} = 0$, otherwise, and so

$$\left[M(\mathcal{R}_d)\, A(\mathcal{G}, \mathcal{R}_d)^{-1}\right]_{ii} = \begin{cases} \alpha_i \left[A(\mathcal{G}, \mathcal{R}_f)^{-1}\right]_{ii} & \text{if } v_i \in \pi(\mathcal{E}_R) \\ 0 & \text{otherwise.} \end{cases}$$

The proof of the lemma follows. □

Remark 9. An in depth analysis of $\left\|G_{\mathcal{G},\tilde{\mathcal{R}}_d}(s)\right\|_2^2$ was undertaken for the specialized class of graphs, namely trees $\mathcal{T}$.[25] To apply some of these results to more generalized connected graphs we consider any spanning tree $\mathcal{T}$ of a connected graph $\mathcal{G}$. In terms of our electrical resistance analogy, the resistor network corresponding to $\mathcal{T}$ is formed by removing resistors from the resistor network corresponding to $\mathcal{G}$. Applying Rayleigh's Monotonicity Principle[b] leads to $\left\|G_{\mathcal{G},\tilde{\mathcal{R}}_d}(s)\right\|_2^2 \leq \left\|G_{\mathcal{T},\tilde{\mathcal{R}}_d}(s)\right\|_2^2$, i.e., the open loop $\mathcal{H}_2$ norm of the system with the coordination graph $\mathcal{G}$ is bounded above by the open loop $\mathcal{H}_2$ norm system with the coordination graph $\mathcal{T}$ corresponding to any of the spanning trees of $\mathcal{G}$.

[b] Rayleigh's Monotonicity Law states that if the edge resistance in an electrical network is decreased, then the effective resistance between any two agents in the network can only decrease.[26]

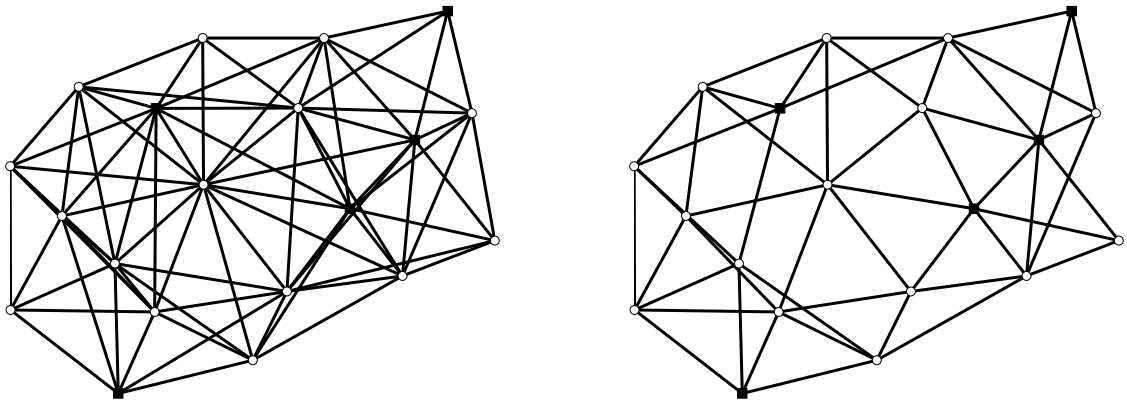

(a) (b)

Figure 3. Agent graph with leader agents (squares). (a) A Euclidean constraint graph (b) A connected subgraph of (a) meeting the global and local edge constraints, $|E| \leq 51$ and $\delta_i \leq 7$ for all $v_i \in V$.

IV. Topology Design

We now consider the design of network topologies that exhibit favorable gust rejection characteristics for sparse and dense swarming. We will proceed to introduce two methods to generate these networks using the open loop $\mathcal{H}_2$ norm as the optimizing metric.

Before continuing we will introduce constraints on the underlying graph structure that are products of the swarming application. Firstly, for all UAVs in the network to reach a common consensus there must be some path connecting each and every UAV along some subset of graph edges, i.e., the graph must be connected. The nodes within the graph represent our UAVs, as no loss or gain of UAVs are assumed the number of nodes n is set. An edge $\{v_i, v_j\} \in E$ in the graph indicates that UAV i is sensing the relative altitude of UAV j and vice versa. The total sensing load on the network is subsequently $2|E|$ and applying an upper bound on $2|E|$ equates to limiting this load. UAV i's sensors can also be limited to a certain quantity of concurrently relative altitude measurements of neighboring UAVs. From a graph-theoretic perspective, this is represented as an upper bound on node i's degree δ_i. Finally, the ability of UAV i to perform accurate relative sensing of UAV j is limited by the Euclidean separation of the two UAVs. A Euclidean based constraint graph can be formed where edges exist between UAVs when they lie in each others sensing range. For topology design, only a subgraph of this constraint graph can be selected. We assume that inter-UAVs distances in the horizontal plane are roughly constant and much greater than the vertical inter-UAV distance, as such the constraint graph is fixed as perturbations in the vertical position do not alter the constraint graph.

Figure 3(a) depicts a Euclidean based constraint graph on 20 nodes. Further, we provide a graph in Figure 3(b) that satisfies the connected Euclidean subgraph constraint with the added global and local load sensing constraints such that $|E| \leq 51$ and $\delta_i \leq 7$ for all $v_i \in V$.

We now have the necessary framework to formulate our methods for network topology design which are MISDP and distributed adaptive network design suitable for sparse and dense swarming, respectively.

A. MISDP Design and Sparse Swarming

As we stated in the background section, the neighborhood of a node v_i in an undirected graph $\mathcal{G} = (V, E)$ is expressed by the entries of the adjacent matrix with $[\mathcal{A}(\mathcal{G})]_{ij} = 1$ when $v_i, v_j \in E$ and $[\mathcal{A}(\mathcal{G})]_{ij} = 0$ otherwise. According to the symmetric property of the adjacent matrix $\mathcal{A}(\mathcal{G})$, a graph with n nodes can use a set of binary variables comprised of $n(n-1)/2$ elements to determine off-diagonal entries of the $\mathcal{A}(\mathcal{G})$ while the diagonals are simply zeros. Using such a framework, we assign binary variable a_{ij} to represent the

element $[\mathcal{A}(\mathcal{G})]_{ij}$ in $\mathcal{A}(\mathcal{G})$ such that

$$\mathcal{A}(\mathcal{G}) = \begin{pmatrix} 0 & a_{12} & \cdots & a_{1n} \\ a_{21} & \ddots & a_{ij} & \vdots \\ \vdots & a_{ji} & \ddots & \vdots \\ a_{n1} & \cdots & \cdots & 0 \end{pmatrix}, \quad a_{ij} = a_{ji},\ (i \neq j). \tag{16}$$

If the cost of constructing a graph with adjacency expressed in Equation 16 is estimated by the number of edge set E, then we can scale the cost by

$$C_E = \sum_{\{v_i, v_j\} \in V} a_{ij}/2; \quad a_{ij} = a_{ji},\ (i \neq j). \tag{17}$$

The degree matrix $\Delta(\mathcal{G})$ of the graph can also be expressed in terms of the binary variables a_{ij} as

$$\Delta(\mathcal{G}) = \begin{pmatrix} \sum a_{1j} & & 0 \\ & \ddots & \\ 0 & & \sum a_{nj} \end{pmatrix}.$$

Therefore the Laplacian $\mathcal{L}(\mathcal{G}) = \Delta(\mathcal{G}) - \mathcal{A}(\mathcal{G})$ is completely determined by the binary variables a_{ij}. We denote the eigenvalues of $\mathcal{L}$ by $0 = \lambda_1(\mathcal{G}) \leq \lambda_2(\mathcal{G}) \leq \cdots \leq \lambda_n(\mathcal{G})$, and quote the following well-known Lemma[2] which can be used to determine the connectivity of the graph.

Lemma 10. *The graph $\mathcal{G}$ is connected if and only if $\lambda_2(\mathcal{G}) > 0$.*

When the network is injected with noise, our goal is to design the topology of the graph by determining the coordination linkages between nodes such that the effective resistance is minimized. At the same time, we want to constrain the construction cost C_E, i.e, the number of edges in the graph. Moreover, the sensing capacity of each node $v_i \in V$ is constrained by the maximum degrees Δ_{maxi}. Finally, the necessary and sufficient condition for a connected graph requires that $\lambda_2(\mathcal{G}) > 0$. In summary, we can formulate the optimal graph design problem as

$$\min_{A(\mathcal{G},\mathcal{R})} \mathbf{tr}(B(\mathcal{R})B(\mathcal{R})^T A(\mathcal{G},\mathcal{R})^{-1}) \tag{18}$$

$$s.t. \qquad a_{ij} = a_{ji}, \quad \forall\, v_i, v_j \in V, \quad i \neq j \tag{19}$$

$$a_{ij} \in \{0, 1\} \tag{20}$$

$$\sum_{i,j=1, i\neq j}^{n} a_{ij}/2 \leq C_E \tag{21}$$

$$\sum_{j=1}^{n} a_{ij} \leq \Delta_{maxi}, \quad v_i \in V \tag{22}$$

$$\lambda_2(\mathcal{G}) > 0 \tag{23}$$

The next step is to transform the objective and constraint functions into linear matrix equalities or inequalities as a MISDP problem. Equations 19-22 are already expressed in linear form. Our concern therefore is with Equations 18 and 23. We first present a linear inequality constraint to ensure the second smallest eigenvalue of graph Laplacian is positive via the following proposition and corollary.

Proposition 11. *For a graph Laplacian $L(\mathcal{G})$ the eigenvalues of $L(\mathcal{G})$ are equivalent to the eigenvalues of $P^T L(\mathcal{G}) P$, where $P = [p_1, p_2, \ldots, p_{n-1}, \frac{1}{n}\mathbf{1}]$ and the unit vector are chosen such that*

$$p_i^T \mathbf{1} = 0, \quad i = 1, 2, \ldots, n-1 \tag{24}$$

and

$$p_i^T p_j = 0, \quad i \neq j. \tag{25}$$

Proof. It is well known the Laplacian $L(\mathcal{G})$ is positive semidefinite matrix and has one eigenvalue equal to zero with related eigenvector $\mathbf{1}$. The eigenvector x associated with the nonzero eigenvalue λ satisfies the following condition

$$x^T L(\mathcal{G}) = \lambda x, \quad \text{for all nonzero} \quad x \in \mathbf{1}^{\perp} \tag{26}$$

where eigenvector x corresponds to a nonzero eigenvalue and is contained in the set of all vectors orthogonal to $\mathbf{1}$, denoted by $\mathbf{1}^{\perp}$. However, without loss of generality, vector x could be the linear combination

$$x = \alpha_1 p_1 + \alpha_2 p_2 + \cdots + \alpha_n p_n,$$

such that $x = Py$ and $y = [\alpha_1, \alpha_2, \cdots, \alpha_n]$ has nonzero elements. Substituting x in Equation 26 one has

$$(Py)^T L(\mathcal{G}) = \lambda Py \Longleftrightarrow y^T (P^T L(\mathcal{G}) - \lambda P) y = 0 \tag{27}$$

Obviously, Equation 27 exists if and only if $P^T L(\mathcal{G}) = \lambda P$. □

Corollary 12. *For a graph Laplacian $L(\mathcal{G})$ the constraint $\lambda_2(\mathcal{G}) > 0$ is equivalent to $L(\mathcal{G}) + \mathbf{1}\mathbf{1}^T/n \succ 0$.*

Proof. It is easy to confirm that the matrix $\mathbf{1}\mathbf{1}^T/n$ has one eigenvalue equal to 1 with corresponding eigenvector of $\mathbf{1}$ and the remaining eigenvalue are all equal to zero. We assume the eigenvectors of matrix $\mathbf{1}\mathbf{1}^T/n$ are denoted by $P = [p_1, p_2, \ldots, p_{n-1}, \mathbf{1}]$ where all elements of P satisfies exact the same condition as stated in Equation 24 and Equation 25. From Proposition 11, one has

$$P^T L(\mathcal{G}) = \begin{pmatrix} \lambda_1(\mathcal{G}) & 0 & 0 \\ 0 & \ddots & 0 \\ 0 & 0 & \lambda_n(\mathcal{G}) \end{pmatrix} P,$$

where $\lambda_1 = 0$ with eigenvector $\mathbf{1}$. We proceed with calculating the eigenvalues of matrix $L(\mathcal{G}) + \mathbf{1}\mathbf{1}^T/n$,

$$P^T (L(\mathcal{G}) + \mathbf{1}\mathbf{1}^T/n) = \begin{pmatrix} \lambda_1(\mathcal{G}) + 1 & 0 & 0 & 0 \\ 0 & \lambda_2(\mathcal{G}) & 0 & 0 \\ 0 & 0 & \ddots & 0 \\ 0 & 0 & 0 & \lambda_n(\mathcal{G}) \end{pmatrix} P.$$

As we assigned $0 = \lambda_1(\mathcal{G}) \leq \lambda_2(\mathcal{G}) \leq \cdots \leq \lambda_n(\mathcal{G})$, $\lambda_2(\mathcal{G}) > 0$ is satisfied if and only if $L(\mathcal{G}) + \mathbf{1}\mathbf{1}^T/n \succ 0$. □

Next, we introduce a slack symmetric matrix $S_{n\times n}$ such that

$$\begin{pmatrix} S & I_{n\times n} \\ I_{n\times n} & A(\mathcal{G},\mathcal{R}) \end{pmatrix} \succeq 0 \Longleftrightarrow S \succeq A(\mathcal{G},\mathcal{R})^{-1}.$$

By minimizing the trace of upper bounds of $A(\mathcal{G},\mathcal{R})^{-1}$, which we relabel matrix S, we simultaneously reach the minima of the desired $\mathbf{tr}(A(\mathcal{G},\mathcal{R})^{-1})$ without performing the nonlinear inverse calculation of $A(\mathcal{G},\mathcal{R})$. The optimization problem proposed from Equations 18-23 is now transformed into a MISDP problem summarized in the following formulation:

$$\begin{aligned} & \min_{A(\mathcal{G},\mathcal{R})} \ \mathbf{tr}(B(\mathcal{R})B(\mathcal{R})^T S) \\ s.t. \quad & a_{ij} = a_{ji}, \quad \forall\, v_i, v_j \in V, \quad i \neq j \\ & a_{ij} \in \{0,1\} \\ & \sum_{i,j=1, i\neq j}^{n} a_{ij}/2 \leq C_E \\ & \sum_{j=1}^{n} a_{ij} \leq \Delta_{maxi}, \quad v_i \in V \\ & L(\mathcal{G}) + \mathbf{1}\mathbf{1}^T/n \succ 0 \\ & \begin{pmatrix} S & I_{n\times n} \\ I_{n\times n} & A(\mathcal{G},\mathcal{R}) \end{pmatrix} \succeq 0 \end{aligned}$$

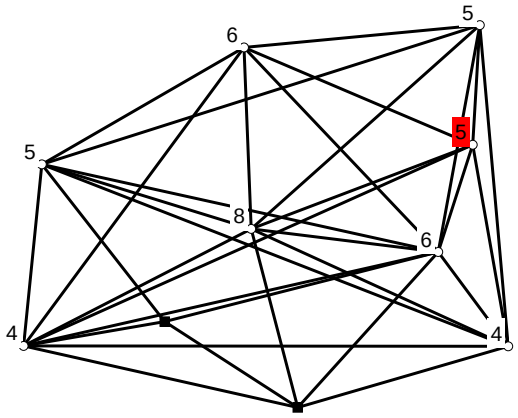

Figure 4. Edge constraint graph with maximum degree constraints indicated. The leader agents (those agents affected by wind gusts) are indicated with squares and the unique degree label corresponds to the agent whose dynamics are displayed in Figure 6.

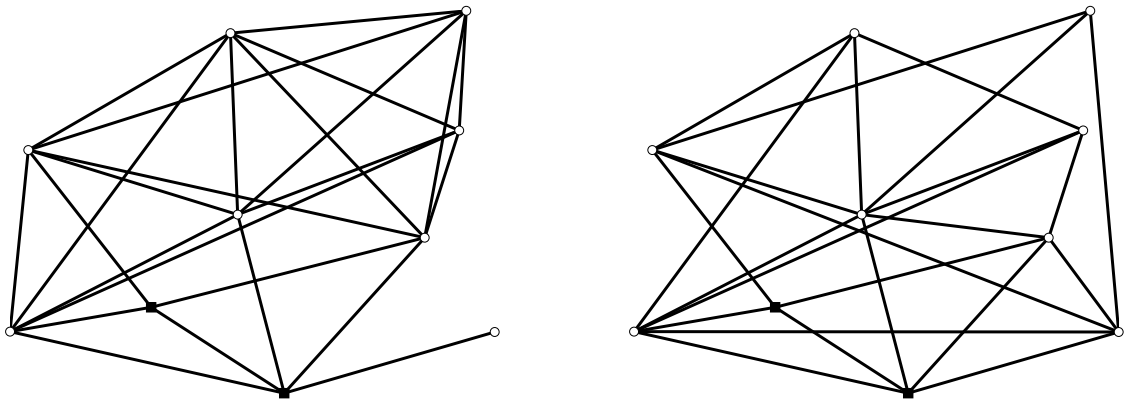

(a) (b)

Figure 5. (a) Original graph and (b) Optimized (adapted) graph both satisfying the edge and degree constraints from Figure 4 with leader agents (squares).

We now apply the above MISDP formulation to the sparse swarming model (8) with 10 UAVs, two of which are acted on by wind gusts. The open loop $\mathcal{H}_2$ norm of the mapping from $q(t)$ to $y(t)$ is $\|G_{\mathcal{G},\mathcal{R}}(s)\|_2^2 = -\frac{1}{2}\mathbf{tr}\left(M(\mathcal{R})A\left(\mathcal{G},\mathcal{R}\right)^{-1}\right)$ (Equation 14). Further, to limit the relative sensing demands on the network, we make the following constraints on the network; that $|E| \leq 25$, $|G|$ must be subgraph of the Euclidean-based constraint graph in Figure 4, and each node has a maximum degree constraints also indicated in Figure 4.

Applying these constraints to the MISDP formulation we acquire the graph in Figure 5 and for comparison a random original graph that meets these constraints is also indicated. The metric $\|G_{\mathcal{G},\mathcal{R}}(s)\|_2^2$ for the optimized and comparative graphs are 1.89 and 2.07 respectively. The output of the UAV marked in Figure 4 was compared in Figure 6 with the constants of model (8) set as $L = 3.49$, $\sigma = 10$, $\bar{h} = 1$, and initial altitudes $x(0) = 0$ and $\bar{x}(0) = 0$.

B. Adaptive Network Design and Dense Swarming

It has previously been demonstrated that leader agents applying a *grounded signal* (all leaders apply a common constant signal) are able to control the mean consensus value of a wind gust disturbed system.[25]

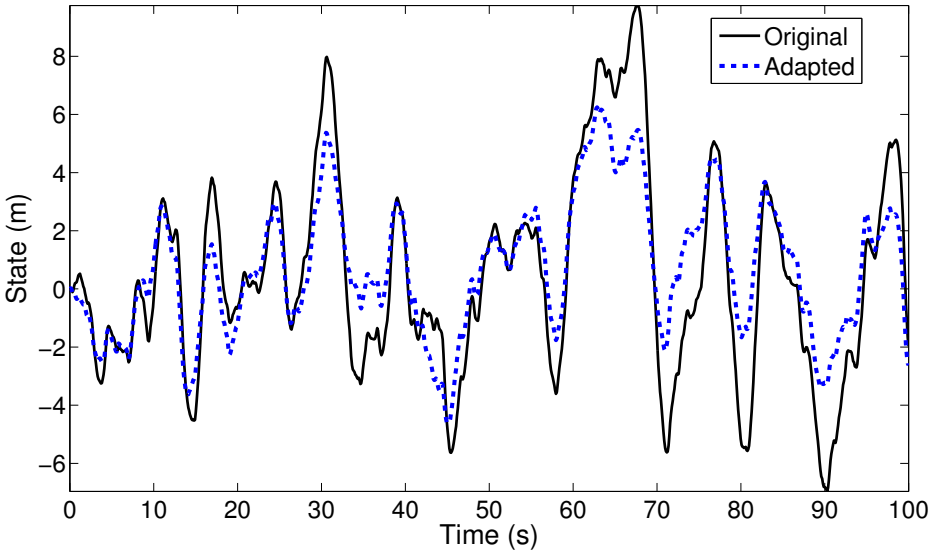

Figure 6. The altitude state of the uniquely marked agent in Figure 4 for the graphs in Figure 5.

We now investigate controlling the consensus value of a wind gust disturbed system using a $\mathcal{H}_2$ control framework *assuming a nominal* $\mathcal{G}$ *in* (10).

A consequence of Proposition 1 is that $A(\mathcal{G},\mathcal{R})$ has only negative eigenvalues. Examining A_w, $\lambda_i(A_w) = -\frac{1}{L}$ for $i = 1, 2$ and as $L > 0$, it follows that A_w has only negative eigenvalues. Therefore the state matrix $\mathcal{A}_D$ is stabilizable and detectable so a stabilizing compensator can be formed.

Hence given a performance measure

$$J = \lim_{t\to\infty} \mathbb{E}\left\{x(t)^T Q x(t) + u(t)^T R u(t)\right\},$$

a compensator that minimizes J can be solved of the form

$$\begin{aligned}\dot{\hat{x}}(t) &= \left(\mathcal{A}_D - \mathcal{B}_D K_c - K_f \mathcal{C}_D\right)\hat{x}(t) + K_f y(t)\\ u(t) &= K_c \hat{x}(t),\end{aligned}$$

where $\hat{x}(t)$ is an estimate of $\begin{bmatrix} x(t)^T & z(t)^T \end{bmatrix}^T$, $K_c \in \mathbb{R}^{r\times n}$ is the compensator gain and $K_f \in \mathbb{R}^{n\times n}$ is the filter gain. The compensator and filter gains satisfy $K_c = R^{-1}\mathcal{B}_D^T P$ and $K_f = S\mathcal{C}_D^T V^{-1}$ and P and S are the solutions of the algebraic Riccati Equations,

$$\begin{aligned}0 &= \mathcal{A}_D^T P + P\mathcal{A}_D + Q - P\mathcal{B}_D R^{-1}\mathcal{B}_D^T P\\ 0 &= \mathcal{A}_D S + S\mathcal{A}_D^T + GWG^T - S\mathcal{C}_D^T V^{-1}\mathcal{C}_D S.\end{aligned}$$

The corresponding optimal performance cost is then

$$J^* = \mathbf{tr}(PK_f V K_f^T) + \mathbf{tr}(SQ). \tag{28}$$

For the dense swarming model (11), the stabilizing compensator was applied to a 40-agent UAV network exposed to wind gusts composed of 3 leaders and 37 followers with parameters; $Q = I_{37\times 37}$, $R = 10I_{3\times 3}$,$V = 0.1I_{37\times 37}$, $H = \mathbf{1}$, $W = 1$, $L = 3.49$, $\sigma = 10$, and initial altitude set as $x(0) = 0$. The network topology is depicted in Figure 7. The performance with respect to the average state and control with a desired altitude hover command ($x(t) = 0$) are compared to the grounded signal control in Figure 8.

We now present a network design protocol to improve the $\mathcal{H}_2$ controller performance. We note that the previous formulation using mixed-integer design is no longer feasible as it equates to maximizing a convex function which is NP-hard. It is with this in mind that we propose an edge trading (rewiring), adaptive topology controller to improve the nominal $\mathcal{H}_2$ performance.

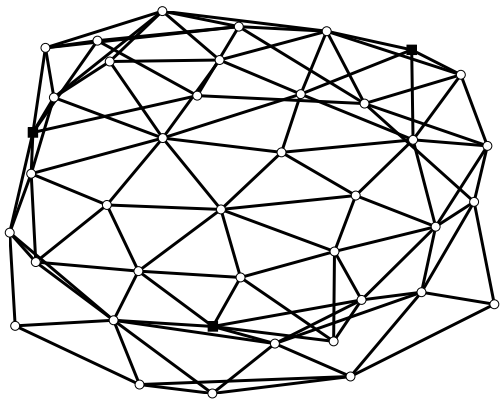

Figure 7. Original agent graph with leader agents (squares).

Protocol 1 Increasing $trP(\mathcal{T},\mathcal{R})$ edge swap

foreach *Agent* v_i **do**
  if $v_k = \mathcal{I}(v_i)$, $\exists v_j \in \mathcal{N}(v_i)$ *and* $v_j \neq v_k$ **then**
    $E \to E - \{v_i, v_j\} + \{v_j, v_k\}$
  end
  if $|\mathcal{I}(v_i)| > 1$, $\exists v_j, v_k \in \mathcal{N}(v_i)$, $v_j \in \mathcal{I}(v_i)$ *and* $v_k \notin \mathcal{I}(v_i)$ **then**
    $E \to E - \{v_i, v_j\} + \{v_j, v_k\}$
  end
end

The protocol runs over the spanning trees of $\mathcal{G}$ with the objective of increasing $\|G_{\mathcal{G},\mathcal{R}}(s)\|_2^2$ via increasing $|\mathcal{E}_R|$ and $E_{\text{eff}}(v_i)$ for all $v_i \in \pi(\mathcal{E}_R)$ as illustrated through Lemma 8. The protocol involves edge trades between neighboring agents executed concurrently and/or in a random agent order while maintaining a connected tree at each iteration. The general procedure is to randomly selected a spanning tree $\mathcal{T}$ of $\mathcal{G}$ and apply **Protocol 1** for some finite number of edge trades and then repeat with a new spanning tree. Within the protocol, we denote edge removal and addition by the set notation "$-/+$", and denote by $\mathcal{I}(v_i)$, the set of all agents that are neighbors of v_i and lie on the shortest path between v_i and any $r_j \in R$. In this direction, let us first define the special set of agents that lie on any of the shortest paths between agents in $\mathcal{R}$ as *main path agents*, i.e., those agents such that are leader or with $\mathcal{I}(v_i) > 1$. The protocol involves two conditions; one to increase the degree of agents in R thus increasing $|\mathcal{E}_R|$ and $\left\|G_{\mathcal{G},\widetilde{\mathcal{R}}_c}(s)\right\|_2^2$, the other to increase the effective resistance for agents in set $\pi(\mathcal{E}_R)$ and thus increasing $\left\|G_{\mathcal{T},\widetilde{\mathcal{R}}_d}(s)\right\|_2^2$. We have previously presented the following lemmas and we refer to reader to Chapman and Mesbahi[24] for the corresponding proofs.

Lemma 13. *Under both conditions of* ***Protocol 1****,* $|\mathcal{E}_R|$ *only increases and the graph remains connected.*

Lemma 14. *For a tree* $\mathcal{T}$*, under the second conditions of* ***Protocol 1****,* $E_{\text{eff}}(v_i)$ for $v_i \in \pi(\mathcal{E}_R)$*, monotonically increases.*

Lemma 13 has the effect of compressing the network about the main path agents. On the other hand, Lemma 14 adds agents to the main path of $\mathcal{T}$ and in doing so elongates the main path.

We now apply the protocol to the dense swarming graph. We restrict the protocol to only edges within the constraint graph displayed in Figure 9(a) and limit the maximum degree of the followers agents at 8. Running the protocol on the graph in Figure 7 over 50 spanning trees, involving 289 edge trades, we produced the final graph displayed in Figure 9(b). The resultant leader-follower model has a $\|G_{\mathcal{G},\mathcal{R}}(s)\|_2^2 = 11.3$ compared to the original system with 4.6. The resultant graph and its response to wind gusts are displayed in Figure 9 and 10. The optimal performance cost J^* as defined in Equation (28) decreased from 14815 to 3265.

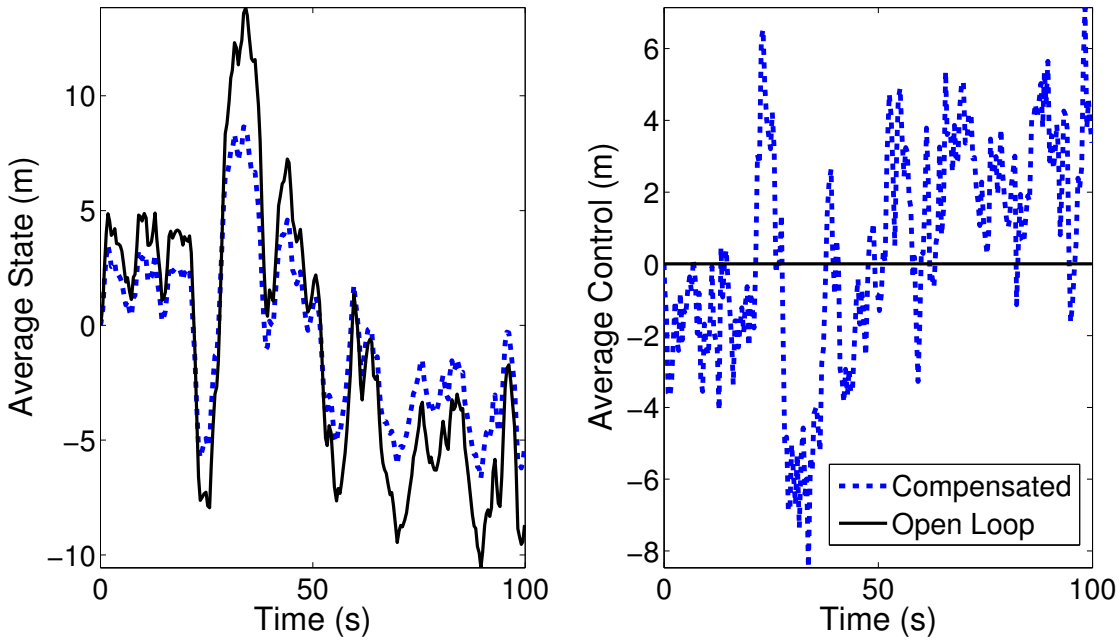

Figure 8. Average state and control over time for the compensated (closed loop $\mathcal{H}_2$ controller) and grounded constant (open loop) control for the wind perturbed graph in Figure 7.

V. Conclusion

The main objective of the present work is to propose a network-theoretic approach for the efficient network topology design of leader-follower systems, specifically UAV swarming in the presence of wind gusts. The open loop $\mathcal{H}_2$ norm was analyzed as a metric to effectively quantify the performance of the underlying network. A MISDP design procedure was formulated accounting for sensing constraints relevant for a sparse swarming application. Similarly, an adaptive rewiring protocol based on the spanning trees of the graph was described for the use in the design of networks for dense swarming with UAV controllers. Both design methods were applied to UAV swarms with notable wind gust rejection improvements.

References

[1]Olfati-Saber, R., Fax, J. A., and Murray, R. M., "Consensus and Cooperation in Networked Multi-Agent Systems," *Proc. IEEE*, Vol. 95, No. 1, Jan. 2007, pp. 215–233.

[2]Mesbahi, M. and Egerstedt, M., *Graph Theoretic Methods in Multiagent Networks*, Princeton University Press, 2010.

[3]Tanner, H. G., Pappas, G. J., and Kumar, V., "Leader-to-Formation Stability," *IEEE Transactions on Robotics and Automation*, Vol. 20, No. 3, 2004, pp. 443–455.

[4]Jadbabaie, A., Lin, J., and Morse, A. S., "Coordination of Groups of Mobile Autonomous Agents Using Nearest Neighbor Rules," *IEEE Transactions on Automatic Control*, Vol. 48, No. 6, 2003, pp. 988–1001.

[5]Stevens, B. L. and Lewis, F. L., *Aircraft Control and Simulation*, Wiley, NJ, 2003.

[6]Mutuel, L. and Douglas, R., "Controller Design for Low Speed Flight in Turbulence," *AIAA Guidance, Navigation, and Control Conference*, 1997, pp. 1111–1121.

[7]Hall, J., "Lateral Control and Observation of a Micro Aerial Vehicle," *45th AIAA Aerospace Sciences Meeting and Exhibit*, No. January, 2007, pp. 8–11.

[8]Shyy, W., Lian, Y., Tang, J., Liu, H., Trizila, P., Stanford, B., Bernal, L., Cesnik, C., Friedmann, P., and Ifju, P., "Computational aerodynamics of low Reynolds number plunging, pitching and flexible wings for MAV applications," *46th AIAA Aerospace Sciences Meeting and Exhibit*, Vol. 24, July 2008, pp. 1–33.

[9]Yang, C.-d., Liu, W.-h., Chang, P.-w., and Weng, H.-j., "Decoupling Control for Hovering Flight Vehicle with Parameter Uncertainties," *AIAA Guidance, Navigation, and Control Conference and Exhibit*, No. 1, 2006, pp. 1–13.

[10]Cheviron, T., "Robust control of an autonomous reduced scale helicopter in presence of wind gusts," *AIAA Guidance, Navigation, and Control Conference and Exhibit*, No. August, 2006, pp. 1–22.

[11]Meskin, N., Khorasani, K., and Rabbath, C. a., "A Hybrid Fault Detection and Isolation Strategy for a Network of Unmanned Vehicles in Presence of Large Environmental Disturbances," *IEEE Transactions on Control Systems Technology*, , No. August, Nov. 2010.

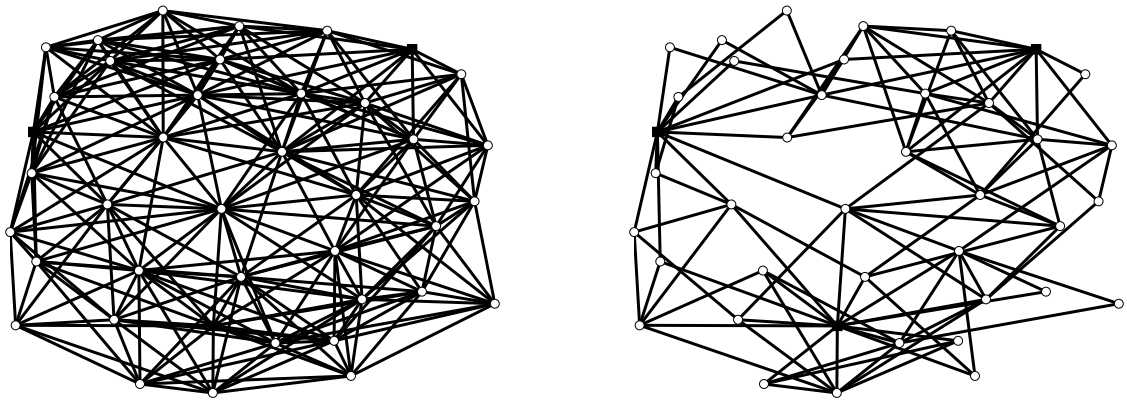

(a) (b)

Figure 9. (a) Edge constraint graph and (b) Resultant leader-follower network after applying Protocol 1 to 50 spanning trees of the graph in Figure 7. The leader agents are marked with squares.

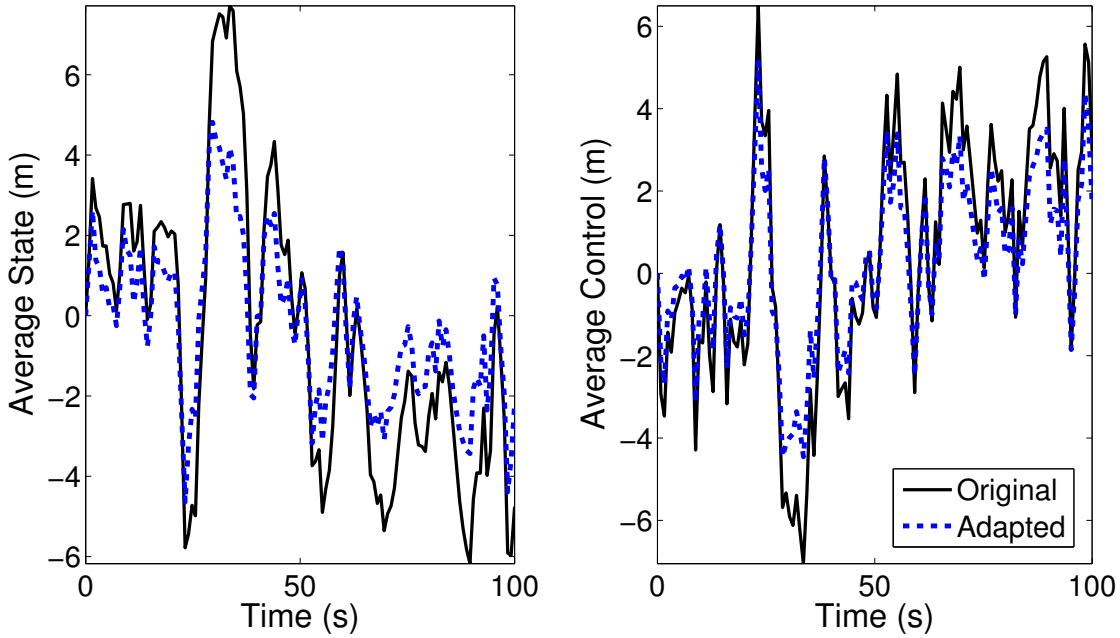

Figure 10. Average state and control over time for the wind perturbed system corresponding to Figure 7 before and after applying Protocol 1.

[12]Olfati-Saber, R., "Flocking for Multi-Agent Dynamic Systems: Algorithms and Theory," *IEEE Transactions on Automatic Control*, Vol. 51, No. 3, 2006, pp. 401–420.

[13]Li, X. and Cao, L., "Largest Laplacian eigenvalue predicts the emergence of costly punishment in the evolutionary ultimatum game on networks," *Physical Review E - Statistical, Nonlinear and Soft Matter Physics, 80(6 Pt 2)*, Vol. 80, 2009, pp. 066101.

[14]Ghosh, A., Boyd, S., and Saberi, A., "Minimizing Effective Resistance of a Graph," *SIAM Review*, Vol. 50, No. 1, 2008, pp. 37–66.

[15]Lofberg, J., "YALMIP : a toolbox for modeling and optimization in MATLAB," *2004 IEEE International Symposium*, 2004, pp. 284–289.

[16]Ghosh, A. and Boyd, S., "Growing Well-connected Graphs," *Proc. of the 45th IEEE Conference on Decision and Control*, IEEE, 2006, pp. 6605–6611.

[17]Zelazo, D. and Mesbahi, M., "Edge Agreement: Graph-Theoretic Performance Bounds and Passivity Analysis," *IEEE Transactions on Automatic Control*, Vol. 56, No. 3, March 2011, pp. 544–555.

[18]Wan, Y., Roy, S., and Saberi, A., "Network Design Problems for Controlling Virus Spread," *Proc. 46th IEEE Conference on Decision and Control*, 2007, pp. 3925–3932.

[19]Kim, Y. and Mesbahi, M., "On Maximizing the Second Smallest Eigenvalue of a State-Dependent Graph Laplacian," *IEEE Transactions on Automatic Control*, Vol. 51, No. 1, Jan. 2006, pp. 116–120.

[20]Wu, Z. and Wang, R., "The Consensus in Multi-Agent System with Speed-Optimized Network," *International Journal of Modern Physics B*, Vol. 23, No. 10, 2009, pp. 2339–2348.

[21]Tyson, G., Lindsay, A. T., Simpson, S., and Hutchison, D., "Improving Wireless Sensor Network Resilience with the INTERSECTION Framework," *Proc. 2nd International Conference on Mobile Lightweight Wireless Systems, Critical Information Infrastructure Protection*, 2010.

[22]Barooah, P. and Hespanha, J. P., "Graph Effective Resistance and Distributed Control: Spectral Properties and Applications," *Proc. 45th IEEE Conference on Decision and Control*, 2006, pp. 3479–3485.

[23]Salsa, S., *Partial Differential Equations in Action: From Modelling to Theory*, Springer, 2008.

[24]Chapman, A. and Mesbahi, M., "Semi-Autonomous Networks: Network Resilience and Adaptive Trees," *Proc. 49th IEEE Conference on Decision and Control*, No. 2, 2010, pp. 7473 – 7478.

[25]Chapman, A. and Mesbahi, M., "Semi-Autonomous Consensus: Network Measures and Adaptive Trees," *IEEE Transactions on Automatic Control (submitted)*, 2011.

[26]Bollobas, B., *Modern Graph Theory*, Springer, New York, 1998.